Research Papers

GREENSUSMATER

Greensusmater
Vol. 2, No. 2, 2025
https://doi.org/10.62755/greensusmater.2025.2.2.36-48

Check for updates

Cross-linking Formation of Taro Starch (Colocasia Esculenta)-Based Hydrogel using Freeze-Thaw Method: Synthesis and Physical Characterization

Halida Rahmi Luthfianti[1], Nuraini Nafisah[1], William Xaveriano Waresindo[1], Asti Sawitri[1], Dian Ahmad Hapidin[1], Fatimah Arofiati Noor[1], Elfahmi Elfahmi[2,3], Dhewa Edikresnha[1,2], Khairurrijal Khairurrijal[1,2,4,5]

[1] *Physics and Technology of Advanced Materials Research Group, Department of Physics, Faculty of Mathematics and Natural Sciences, Institut Teknologi Bandung, Jalan Ganesha No. 10, Bandung, Jawa Barat 40132, Indonesia*
[2] *Bioscience and Biotechnology Research Center, Institut Teknologi Bandung, Jalan Ganesa 10, Bandung 40132, Indonesia*
[3] *Department of Pharmaceutical Biology, School of Pharmacy, Institut Teknologi Bandung, Jalan Ganesa 10, Bandung 40132, Indonesia*
[4] *Department of Physics, Faculty of Science, Institut Teknologi Sumatera, Jalan Terusan Ryacudu, Lampung Selatan 35365, Indonesia*
[5] *Center of Green and Sustainable Materials, Institut Teknologi Sumatera, Jalan Terusan Ryacudu, Lampung Selatan 35365, Indonesia*

Corresponding author: krijal@itb.ac.id; dhewa@itb.ac.id

ARTICLE HISTORY: Received: July 1, 2025 | Revised: September 22, 2025 | Accepted: September 29, 2025

ABSTRACT

This study successfully made starch from taro tuber flour using immersion methods (AQ, SM) and centrifugation methods (CE). Taro starch with the AQ method produced the most starch content, thus improving the viscosity parameter in the pasting properties test. A simple mathematical model was used to control the taro starch pasting process and product. The highest R-value in the AQ sample was 309.88 s, indicating the strongest starch granule resistance. Meanwhile, the S-value in this study showed that all samples were above 1, which indicated that water penetration affected the swelling rate of starch granules. Taro starch with different isolation methods was analyzed for hydrogel formation using optical microscopy, SEM, swelling degree test, weight loss, color analysis, and texture profile analysis (TPA). The morphological images show three phases of a taro starch hydrogel formation: granular, potential cross-linking, and cross-linking hydrogel with a firm structure. Optimization of freeze-thaw process parameters was carried out to determine the optimum parameters of starch hydrogel formation, which was obtained under freezing conditions for 17 hours at -23°C and thawing for 7 hours at 4°C. The sample CE resulted in the most stable hydrogel formation, showing the highest amylose content, protein content, and the lowest impurities or ash content. The CE starch concentration of 10% resulted in the highest swelling degree and the lowest weight loss, indicating that the ability of the hydrogel to maintain its structure was stronger and more elastic. The textural properties of CE hydrogel at a concentration of 10% showed the most stability. It had the highest hardness, fracturability, chewiness, and springiness. Physical characteristics showed that the starch hydrogels had a dense, porous surface and formed a cross-linking structure. It can potentially be used in functional food applications to control the release of bioactive compounds..

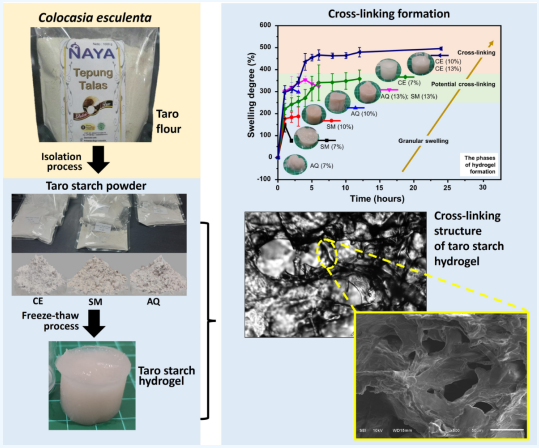

Keywords: *Taro starch, Hydrogel, Cross-linking Formation, Functional Food*

1. INTRODUCTION

Taro, scientifically known as Colocasia esculenta, is classified as a minority or orphan crop within the tuber category. Although not commonly traded worldwide, it is crucial to regional food security [1, 2]. Orphan crops provide carbohydrates, resistant starch, protein, minerals, potassium, vitamins, and dietary fiber. These nutrients can enhance nutrition and maintain food security [3, 4]. People worldwide consume rice, corn, and wheat; taro has yet to be fully utilized to address chronic malnutrition. However, the limited variety of foods indicates a potential danger to nutritional stability worldwide [5, 6]. Efforts to enhance food security through functional food innovations, particularly in food products fortified with nutraceutical content, are gaining attention. Grand View Research reported that the global market for functional food products reached USD 280.7 billion in 2022. The value is projected to rise to USD 586.1 billion by 2030 [7].

In 2021, hydrogel-based functional food products were marketed to reach approximately USD 9,928 million [8]. Hydrogels, which are 3D materials composed of polymer cross-linking networks, play a crucial role in our research on taro hydrogel-based functional foods. Traditionally, many hydrogels have been produced from synthetic polymers. However, our team's previous research has successfully developed hydrogels from polyvinyl alcohol (PVA) loaded with bioactive compounds, demonstrating their potential for nutraceutical functions in biomedical applications [9–13]. Although there has been some development, there is a crucial need to evaluate hydrogels for future food applications, considering environmental issues, toxic materials, and expensive materials. Finding alternative polymers that are more suitable, such

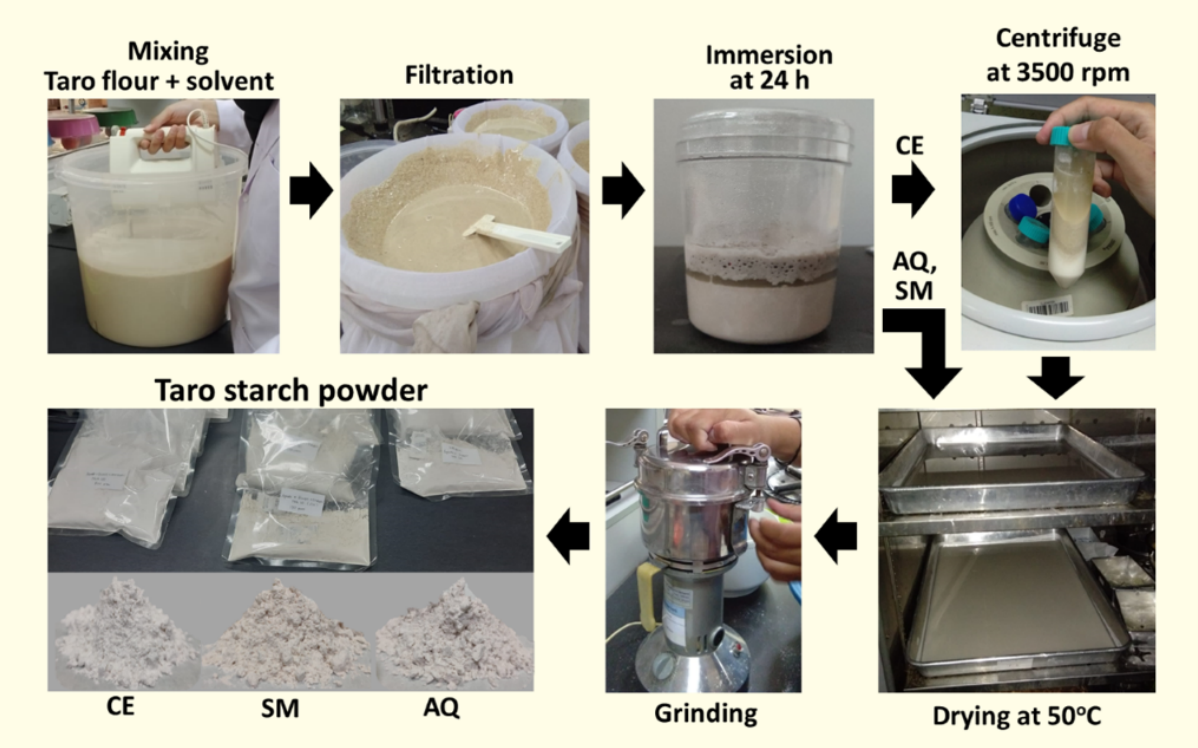

Figure 1. Isolation process of taro starch

as natural ones, is not just a challenge but a significant step towards a sustainable and healthy food industry. Taro starch is included in the category of safe starch, which can improve gastric health and help control blood sugar [3]. In addition, taro starch can be a source of natural polymers to synthesize environmentally friendly hydrogels. So, it can be used as a source of polymers to improve body health. In its utilization, the concentration of natural polymers, mainly taro starch, depends on the isolation method. The presence of amylose and amylopectin in different contents will impact the composition of the hydrogel, hence influencing its structure [14]. High amylose content leads to the firm and elastic structure possessed by taro starch hydrogel. This structure enhances its stability, particularly in water, as the high amylose content resists water solubility and structural degradation [15]. Compared with other starches (e.g., potato, corn), taro starch can produce high amylose content with a simple isolation method.

In contrast, corn and potato starches obtain high amylose content with modified isolation methods. Corn and potato starches with high amylopectin and low amylose content can produce hydrogels that retain water but have low stability because they are more susceptible to disintegration in water [25, 26]. Regarding functional properties, taro starch products offer advantages in applications requiring sustained release, encapsulation, or biomedical uses, due to their enhanced mechanical strength and structural stability. Potato and corn starches, with their softer and more water-absorbent gels, are better suited for applications where rapid swelling, hydration, or a softer texture is desired, such as in food texturizing and cosmetics [15, 27, 28].

The starch isolation process is a critical step that defines the functional characteristics of starch and has a fundamental influence on hydrogel formation [16]. Conventional and enzymatic methods are typically used to isolate taro starch. Conventional techniques involve immersing and centrifuging with solvents such as sodium hydroxide (NaOH), calcium carbonate ($CaCO_3$), distilled water, sodium chloride (NaCl), or sodium metabisulfite ($Na_2S_2O_5$). Distilled water and sodium metabisulfite are widely used as solvents in the food industry [29, 30]. The precipitate from the immersion process is manually isolated to obtain starch powder. In contrast, the precipitate obtained from the centrifugation process is separated using a centrifuge. On the other hand, using enzymes in the process may result in the material becoming contaminated when it is used as a functional food [31]. Considering toxicity concerns, the conventional method of isolating taro starch is preferable due to its simple process and ability to produce starch with high purity [32].

Therefore, this research focuses on analyzing the formation of hydrogels in samples with taro starch isolation using the immersing method (distilled water and sodium metabisulfite) and the centrifugation method. The isolation method with the highest purity of starch was then synthesized into hydrogels at various concentrations. Then, the swelling degree, weight loss, optical microscopy, scanning electron microscope (SEM), color analysis, and texture profile analysis (TPA) were characterized to determine the formation of the hydrogel structure. The hydrogel structure is composed of cross-linking between polymer chains. The cross-linking method used in this study for taro starch hydrogel is a freeze-thaw method. This physical cross-linking method is a green synthesis, which has simple, economical, and non-toxic characteristics [33]. So, it has the potential to produce hydrogels as a matrix for functional food.

Table 1. Proximate characteristics of taro starch with different isolation methods according to the references [16–24]

Sample	Starch (%)	Amylose (%)	Fat (%)	Protein (%)	Ash (%)	Moisture (%)
AQ	98	20.7	0.23	0.23	0.24	10.43
SM	84.2	11.58	0.26	0.19	0.94	13.6
CE	87.68	30.62	0.27	1.46	0.28	11.5

Table 2. Pasting properties of taro starch with various isolation methods.

Sample	PT (°C)	PV (mPa.s)	HV (mPa.s)	FV (mPa.s)	BV (mPa.s)	SV (mPa.s)
AQ	85.17	1575	957	2183	618	1226
SM	90.47	775	265	663	510	398
CE	86.42	1031	423	813	608	390

2. METHODS

2.1 Materials

Taro flour was obtained from CV Primanaya, Indonesia for taro starch isolation. The distilled water and sodium metabisulfite ($Na_2S_2O_5$, food grade) were purchased from PT Brataco Chemistry, an Indonesian supplier. The phosphate-buffered saline (PBS) solvent was acquired from the School of Pharmacy ITB (Institut Teknologi Bandung) in Bandung, Indonesia.

2.2 Taro Starch Isolation and Hydrogel Synthesis

Starch isolation was carried out with reference to Ahmed et al. [32] and Vithu et al [16], with slight modifications, including an immersion method using distilled water (AQ), sodium metabisulfite (SM), and a centrifugation method (CE). SM and AQ methods were simple with a 2:5 (w/v) blend of taro powder in 1% $Na_2S_2O_5$ solution and distilled water (10 g/30 mL). After cheesecloth filtering, the liquid was sedimented for 24 hours at room temperature. All suspended impurities were removed using distilled water, and the residue was dried at 50°C for 12 hours to make starch powder. The CE method used a 3500-rpm centrifuge to separate the sediment. The dry powder, after centrifugation, was crushed in a mortar and screened through an 80-mesh screen for fine taro starch powder. The isolation process of taro starch was summarized in Figure 1.

Taro starch hydrogel was started by optimizing the freeze-thaw process parameters, including freezing-thawing time for 16-8 hours (a), 17-7 hours (b), 20-4 hours (c), respectively, with freezing/thawing temperature of samples a and b of -23/4°C, while sample c was -23/37°C. The great freeze-thaw parameters (the highest swelling degree, the lowest weight loss) were then fabricated with variations in taro starch concentration of 7%, 10%, and 13% (w/w) in different isolation methods (AQ, SM, CE). Starch was dissolved in distilled water and stirred at 100°C for 2 hours. After viscous and gelatinization, the precursor solution was frozen and thawed with parameter b, resulting from optimizing before: freezing for 17 hours at -23 °C and thawing for 7 hours at 4 °C. This freeze-thaw process was done for four cycles. The schematic of taro starch hydrogel synthesis is illustrated in Figure 2a.

2.3 Characterization of Taro Starch

Taro starch paste was characterized and modeled using Rapid Visco Analyzer (model RVA-4, Newport Scientific, Australia) with Standard Analysis 1 profile. The paste parameters obtained were pasting viscosity (PV), holding viscosity (HV), pasting temperature (PT), final viscosity (FV), breakdown viscosity (BV), and setback viscosity (SV). For mathematical modeling analysis, according to Palabiyik et al., in the four model parts [34]: The first part, Eqn (1)'s modified Hill model, explains the first part of the curve's beginning area to PV.

$$V = \frac{PV \times t^S}{R^S + t^S} \tag{1}$$

V is viscosity (mPa.s), t is time (s), R is time to reach 50% of PV (s), and S is starch coefficient, which measures starch swelling. S>1 implies that water entry into starch granules accelerates swelling. If S<1, starch granule swelling is prevented, and if S=1, water infiltration does not cause swelling.

The second component is explained by Eqn (2)'s Arrhenius model. It's in PV till the temperature peaks before stabilizing.

$$\eta = A_0 \exp\left(\frac{E_a}{RT}\right) \tag{2}$$

η,A_0, E_a,R, dan T represent viscosity (mPa.s), Arrhenius model constants, gas constant (8.314 J/mol.K), and temperature (K). The third part is the exponential model in Eqn (3), which explains the steady temperature third component. η represent viscosity (mPa.s), t represent the time during the third part model (s), K and n are model parameters.

$$\eta = K \exp(nt) \tag{3}$$

The fourth part is similar to the second part model with Eqn (2).

The formability of the hydrogels was evaluated using an optical microscope, SEM, swelling degree, weight loss, color analysis, and TPA. The internal morphology of the hydrogels was analyzed using an optical microscope and SEM by cutting the hydrogels transversely. Magnification of 10x was performed using AmScope MUI1000, United States, and 5000x was performed using SEM (JEOL, JSM-6510LA, USA).

The swelling degree was also investigated to see the behavior of the hydrogels when exposed to liquids. This test was conducted by immersing the hydrogel in a phosphate-buffered saline (PBS) solution for 48 hours. Previously, the hydrogel was dried for three days at 50°C to evaporate the water, then weighed and referred to as W_0. Throughout the testing procedure, the hydrogel was weighed at intervals, precisely at 0, 3, 6, 9, 12, 24, and 48 hours, and labeled as W_t.

Table 3. Mathematical modelling of pasting curve with various isolation methods of taro starch.

Sample	1st part			2nd part		3rd part		4th part	
	R	S	R^2	E_a	R^2	K (Pa·s)	R^2	E_a (kJ/mol)	R^2
AQ	309.88	16.42	0.9984	N.A	N.A	7.57	0.9968	78.90	0.9828
SM	304.59	26.47	0.9905	N.A	N.A	15.33	0.9954	92.06	0.9762
CE	306.92	16.64	0.9975	N.A	N.A	8.79	0.9817	95.86	0.9297

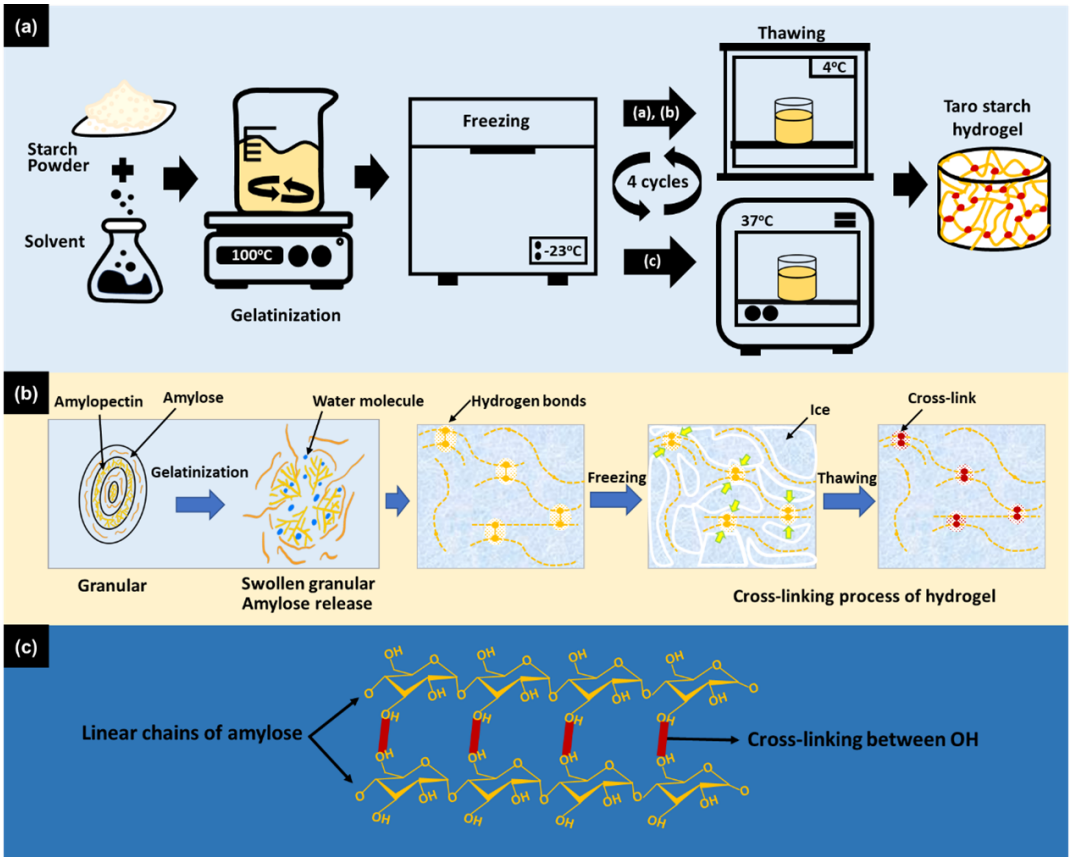

Figure 2. Schematic of taro starch hydrogel (a) synthesis process, (b) molecular information, and (c) cross-linking formation between OH groups

The ratio between the weight before and after immersion is calculated as the swelling degree shown by Eqn (4).

$$Swelling\ degree = \frac{W_t - W_0}{W_0} \times 100\% \quad (4)$$

The soaked hydrogel was then dried again for three days at 50 °C and weighed as W_1 to see the weight loss of the starch hydrogel. Weight loss can be calculated by Eqn (5).

$$Weight\ loss = \frac{W_0 - W_1}{W_1} \times 100\% \quad (5)$$

The color analysis of starch hydrogel was analyzed using starch photographs, using the bivariate histogram approach with the PULUZ foldable LED Ring Light Studio and Nikon D3100 camera. The software used for analysis was ImageJ (version 64-bit Java $1.8.0_172$, NIH, USA), which provided white-level histograms [35].

The texture of the hydrogel can be analyzed using TPA tests conducted with a texture analyzer (TA. XTExpress, Stable Micro Systems). The hydrogel samples were dehydrated using a dehydrator at 50°C for 12 hours. This test was conducted by pressing the hydrogel using a cylindrical P36 probe with a diameter of 36 mm so that the amount of adhesiveness, hardness, springiness, cohesiveness, gumminess, chewiness, and resilience could be obtained.

3. RESULTS AND DISCUSSION

Taro starch with different isolation methods resulted in the proximate characteristics shown in Table 1. Samples with the AQ method produced the highest starch content because distilled water is a polar solvent that effectively dissolves other polar solutes, such as ash and other impurities, in taro samples. These impurities can be easily dissolved and separated from the starch to produce a purer isolate. In addition, starch is a polysaccharide that tends to be hydrophobic and insoluble in water at room temperature. Taro starch will precipitate, while other components soluble in distilled water remain in the liquid phase.

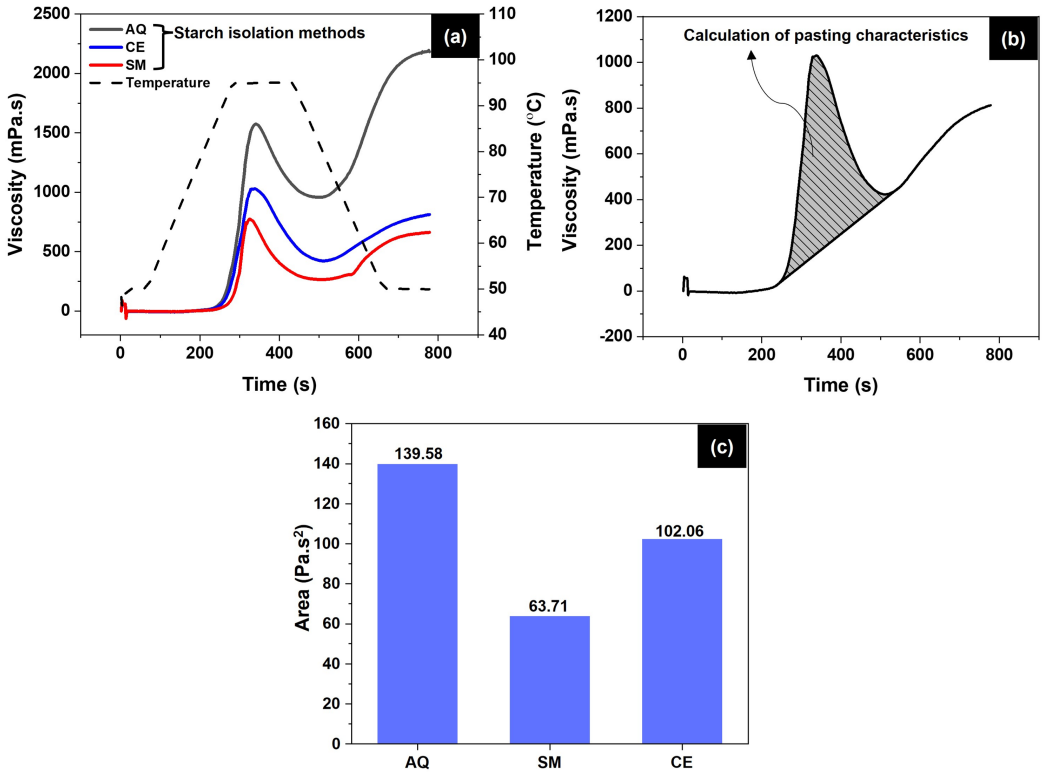

Figure 3. (a) Pasting curves of AQ, CE, and SM hydrogels, (b) the area under the viscosity versus time curves, and (c) the area values of AQ, CE, and SM hydrogels

The AQ method facilitates the separation of starch from other components. Distilled water does not react with starch or cause chemical degradation of its structure, as may occur with other chemical solvents. As a result, it helps preserve starch content during the isolation process [36, 37]. In contrast, the SM isolation method contains sulfur that can bind with minerals contained in taro starch, such as calcium, magnesium, or potassium, and form sulfate compounds. The sulfate compounds will bind to the taro starch and cause an increase in the ash content of the taro starch [38].

The CE isolation method showed the highest amylose content of 30.62% [24]. Centrifugation is a method of extracting taro starch by separating starch particles with other components based on their specific gravity. Amylose has a smaller molecular size than amylopectin, so amylose is more easily separated from other components. The separated amylose then collects at the bottom of the centrifuge container and causes high levels of amylose. The higher amylose content and the lower amylopectin content, the better the hydrogel synthesis process will have physical properties as a conducting matrix [39].

3.1 Pasting Properties of Taro Starch

Starch gelatinization is one of the interesting characteristics to be discussed. During the gelatinization process, a phase transition occurs that is stimulated by the starch suspension being heated in water, resulting in granule swelling. This reduces crystallinity and releases amylose from the starch granules. The resulting hydrogen bonds between the OH groups of amylose and amylopectin, which change the properties of the paste, as shown by the amylograph curve (Figure 3) [40]. Amylograph characteristics are influenced by several factors, including granular morphology, starch content (amylose/amylopectin), and non-starch components such as phosphorus, lipids, and proteins [41].

Figure 3a shows the curve of the change in viscosity of starch against time during temperature increase and decrease. This curve shows the characteristics of taro starch with different isolation methods. Pasting temperature (PT), pasting viscosity (PV), holding viscosity (HV), final viscosity (FV), breakdown viscosity (BV), and setback viscosity (SV) represent the properties of the starch paste [42]. The specific values of the starch paste properties are summarized in Table 2. The PT is the temperature at which the viscosity of starch starts to rise, indicating the onset of starch granule gelatinization. Due to increased temperature, water is absorbed into the starch granules in the gelatinization process. The higher moisture content was the higher the PT, which indicates a longer absorption process. The SM method showed the highest moisture content of about 13.6% and the highest PT value. The sample with the AQ isolation method showed the lowest moisture content of about 10.46% [17, 22].

PV is influenced by fat and starch content. During gelatinization, the presence of fat leads to the formation of starch-fat complexes around the granules, making it more difficult for water to be absorbed into the granules [41]. Furthermore, the PV value is influenced by the starch content as the rise in viscosity during the gelatinization process is a result of the swelling of starch granules [43, 44]. The AQ method with the lowest lipid and highest starch content has the most significant PV, suggesting a more rapid gelatinization process.

The parameters SV and FV are related to the retrogradation process of starch granules. SV indicates that the starting point of viscosity increases again during the retrogradation

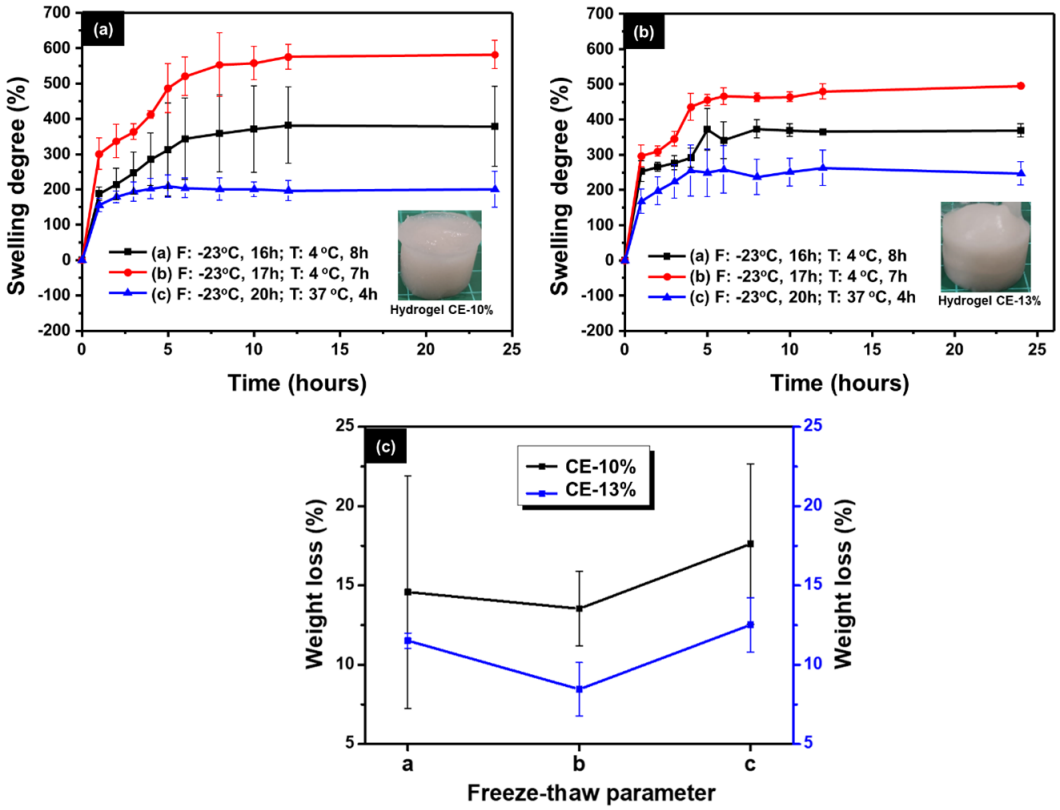

Figure 4. Evaluation of freeze-thaw parameters of taro starch hydrogel (a) swelling degree at concentration 10%, (b) swelling degree at concentration 13%, (c) weight loss at concentration 10% and 13%.

process. Meanwhile, FV relates to the final viscosity after the process. Both describe the retrogradation ability of starch, which depends on the starch content (amylose and amylopectin) [34]. The AQ method with the highest SV and FV values demonstrated the most uncomplicated retrogradation process. The retrogradation process includes the cross-linking of molecules that contain amylose and amylopectin.

HV is the viscosity of starch granules disrupted during shearing and heating. Starch granules become increasingly susceptible to shear and heat disintegration as they swell, especially in starches with lower amylose content [45, 46]. Amylose is released from the granule during the gelatinization process. When amylose is small, the susceptibility of the granule to disintegration is smaller, as shown in the sample using the SM method. BV is correlated with swelling capacity, temperature stability, and the ability of starch granules to maintain their structure [47]. AQ, with the highest BV value, shows a firmer structure and superior starch granule integrity. In contrast, SM, with the lowest BV value, exhibits the lowest strength and stability. This is directly proportional to the starch content in each sample, according to the reference in Table 2.

The area under the viscosity versus time curve (Figures 3b-c) depicts the state of the starch sample from liquid-paste-gel during the gelatinization and retrogradation processes. It can be helpful to control the starch product by considering the amylose and amylopectin content [48, 49]. The AQ sample with the highest starch content showed the highest area of 139.58 Pa.s^2, indicating the stability of the sample in paste form. On the other hand, in the SM sample, the shape of the sample changes quickly to either liquid or solid again.

Simple mathematical modeling was conducted to analyze product development and starch characteristics, such as understanding how quickly the viscosity peak is reached to determine the processing time for product manufacturing. In addition, it can understand the swelling kinetics of starch granules during the gelatinization process and predict various parameters such as starch texture and rheological properties, which are helpful for quality control and product processing design [34, 43]. The pasting curve is segmented into four sections of mathematical models and quantitatively shown in Table 3. In the initial model, the R-value represents the time at which the viscosity hits 50%. This measurement is useful for examining the resistance of the starch to gelatinization and retrogradation processes [43]. The AQ method with the highest starch content exhibited a higher duration for granule disintegration, measuring 309.88 s, followed by CE and SM at 306.92 s and 304.59 s, respectively. The S-value in this model is the starch coefficient, which indicates the swelling rate. Regarding our result, the entry of water into the starch granule increases the swelling rate of the granules as S>1 for all starch samples. The SM method has the highest S of 26.47, followed by CE and SM of 16.64 and 16.42, respectively. These findings are consistent with prior research, which found that starch amylose content is inversely related to S-value. R-value and S-value are related to the gelatinization process, which involves hydrogen bond breaking in the amorphous part and water absorption related to granule swelling in the amorphous region [34, 50].

The second model shows granule degradation as the temperature increases. The curve obtained from this study did not fit the model because the granule degradation indicated

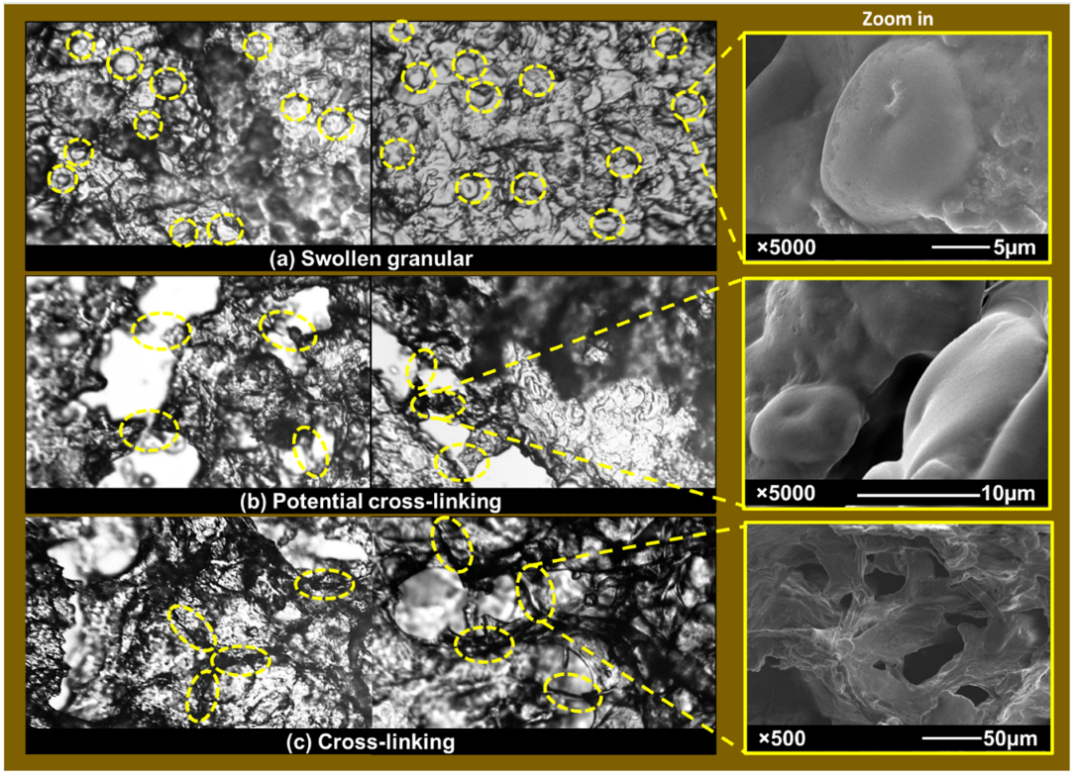

Figure 5. Optical microscope images of the hydrogel formation phase (a) granular swelling, (b) potential cross-linking, (c) cross-linking, and SEM images for zoomed in

by the viscosity decrease occurred when the temperature was already stable. This phenomenon aligns with prior studies finding that in corn and wheat samples that have reached a stable temperature state at maximal viscosity, it is not fit using this model [34]. In the third model, the K-value relates to the viscosity influenced by amylopectin [51]. The high content of amylopectin leads to reduced stability of starch as the swollen granules during stirring and heating [34]. The SM method with the highest amylopectin content and the lowest amylose content has a K-value of 15.33 Pa.s, indicating the lowest starch stability. The coefficient of determination (R^2) for this model varied between 0.9817 and 0.9954, which implies a high level of accuracy in fitting the curve presented in Figure 3a.

In the fourth model, Ea correlates with the rate of retrogradation. Upon cooling, amylose molecules within the starch granule interact with amylopectin, resulting in the formation of a solid structure [34]. The sample with the highest amylose concentration exhibited the highest activation energy (Ea) value and retrogradation rate.

3.2 Macro-microscopic Analysis of Taro Starch Hydrogel Formation

The macro-micro properties of hydrogel formation are influenced by the amylose-amylopectin ratio. The ratio of amylose/amylopectin is crucial in determining the textural properties and stability of starch-based hydrogels. The high amylose content in hydrogels forms dense and rigid structures with low water absorption and increased stability, making them ideal for applications requiring firm and durable gels. During freezing, amylose chains released from the granules are compressed by ice crystals, promoting the formation of hydrogen bonds. Upon thawing, the remaining free hydroxyl groups establish additional bonds (Figure 2b). Hydrogen bonds of the linear amylose chains form a cross-linking hydrogel network (Figure 2c). In contrast, hydrogels with higher amylopectin content have a more porous structure, facilitating enhanced water absorption and resulting in softer, less firm gels that tend to disintegrate more easily in water [34, 39]. These differences allow the amylose-amylopectin ratio to control properties suitable for various applications.

Table 4. Hydrogel formation based on variations in freeze–thaw parameters, isolation methods, and taro starch concentration.

Isolation method of taro starch	Concentration of taro starch (wt%)	Freezing: −23°C, 17 h, Thawing: 4°C, 7 h
Immersion with distilled water solvent (AQ)	7	×
	10	×
	13	o
Immersion with $Na_2S_4O_5$ solvent (SM)	7	×
	10	×
	13	o
Centrifuge (CE)	7	o
	10	✓
	13	✓

×: no hydrogel formed; o: hydrogel formed with brittle structure; ✓: hydrogel formed with firm structure.

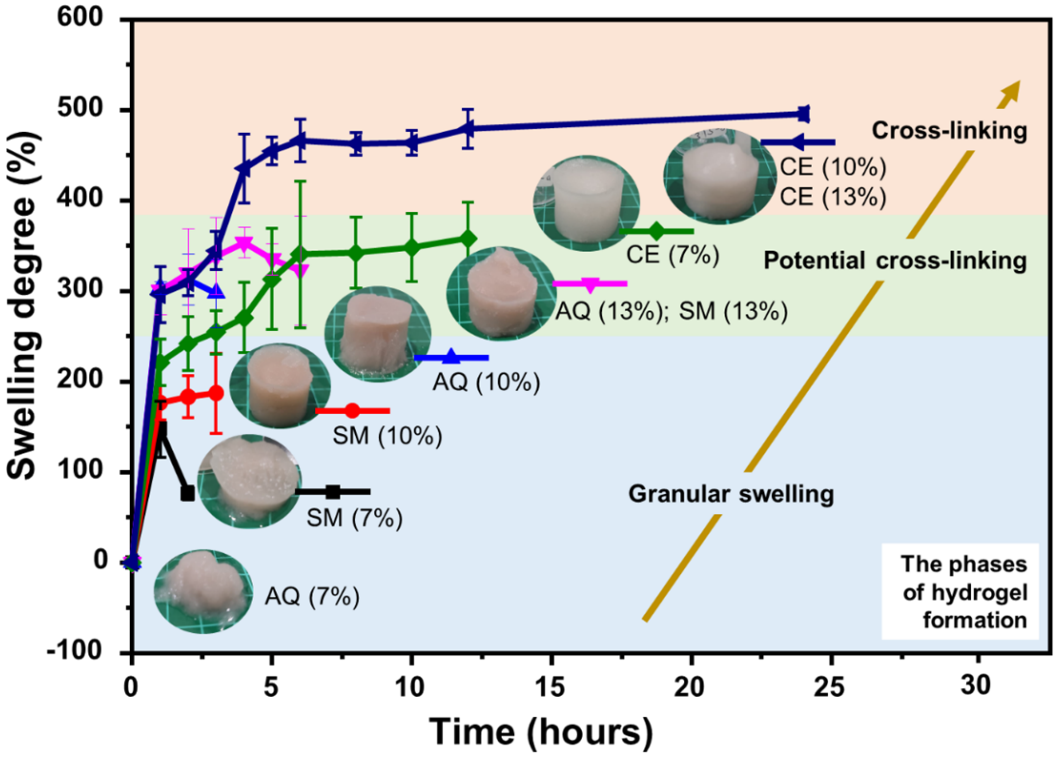

Figure 6. Formation of taro starch hydrogel with swelling degree test.

Figures 4 show the freeze-thaw parameter optimization of CE hydrogel using swelling degree and weight loss analysis. A higher degree of swelling and weight loss represents good structural integrity as a delivery platform. The concentrations used were 10% and 13% (w/w). The swelling degree is related to the hydrogel's ability to swell, which can be used in the loading and controlling release of nutraceuticals [52], and can help reduce hunger by enlarging as it traverses the digestive system [48]. Swelling can be tuned through process parameters including polymer composition, cross-linking density, porosity, and external stimuli (pH, ionic strength, temperature). The advantage of swelling-controlled release is that it allows for tuning of the release profile by adjusting the hydrogel design parameters [52]. While weight loss reflects the structural stability and degradation profile of the hydrogel. Controlled degradation is essential for transient delivery systems, where excessive weight loss ensures network erosion and can compromise structural integrity and lead to burst release, which is undesirable for precise dosing [9]. According to our results, the sample with the parameters of freezing for 17 hours at -23 °C and thawing for 7 hours at 4 °C produced the highest swelling degree and the lowest weight loss, which are the most optimum parameters for hydrogel formation. In contrast, freezing for 20 hours at -23 °C and thawing for 4 hours at 37 °C showed the lowest swelling degree and the highest weight loss. The swelling degree and low durability of the hydrogel structure at 37°C thawing conditions were caused by the extreme temperature during the thawing process. At the same time, the starch chain (amylose/amylopectin) is a long polymer chain that requires a longer cross-linking process to produce a stronger cross-link at a lower thawing temperature (4 °C) [53].

Moghadam et al. (2022) reported that a starch-based hydrogel as a drug delivery system, composed of PEG and loaded with quercetin, showed a swelling degree of 103-140% [54]. Another study reported a swelling degree of starch/polyacrylamide/gelatin composite hydrogels of around 500% [55]. In this study, the taro starch hydrogel synthesis process is presented without adding other polymer reinforcements, and it is an environmentally friendly method. Taro starch hydrogel successfully achieved a swelling degree of 150-500%. The highest swelling degree is helpful for the controlled release of nutraceuticals, so taro starch hydrogel has the potential as a delivery system.

Table 4 shows the formation of hydrogels macroscopically with different starch isolation methods and different starch concentrations. Hydrogels formed with brittle structures have a swelling degree of less than 12 hours, while hydrogels formed with firm structures can swell beyond 12 hours. The viscosity of the paste has a significant impact on the formation of hydrogels during the gelatinization process. However, in this case, the sample has not thickened sufficiently to become a paste. Amylose, a fundamental factor in the formation of hydrogel structure, significantly impacts the viscosity throughout the gelatinization process [41]. In the CE isolation method, formation began at a starch concentration of 7%, while in the AQ and SM isolation methods, formation began at a starch concentration of 13%. The CE isolation method might have a higher amylose content (in reference to Table 2) as a cross-linking agent for the hydrogel structure.

Figure 5 shows the hydrogel formation process to explain Table 4 with a microscopic analysis. The formation of hydrogel, shown in the morphological structure of optical microscope and SEM images, is divided into three phases: granular swelling, potential cross-linking, and cross-linking phases. The granular swelling phase indicates unformed

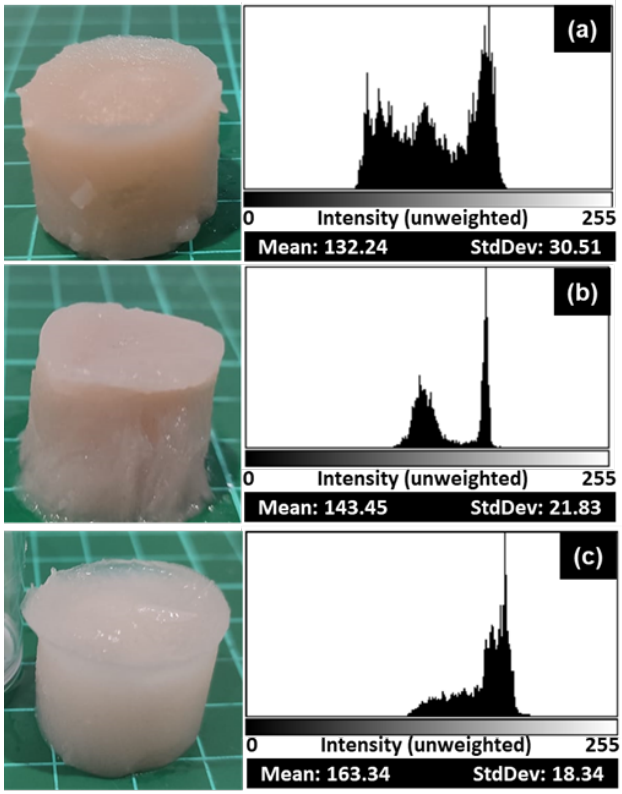

Figure 7. Color analysis of taro starch hydrogel with various isolation method (a) SM, (b) AQ, (c) CE.

hydrogels (Figure 5a), where starch granules expand due to gelatinization. These phases are observed in samples with SM and AQ isolation methods at 7% and 10% concentrations. As studied in previous research, swelling of granules occurred in native starch that was not prepared with the cross-linking process [32, 56]. In addition, the potential cross-linking phase indicates that hydrogels formed with a brittle structure have begun to show porosity (Figure 5b). These potential cross-linking consist of amylose at low concentrations, where the O-H bonds are weak to form stable bindings. The potential cross-linking phases were observed in samples with AQ and SM isolation methods at a concentration of 13% and in samples with the CE isolation method at a concentration of 7%. Finally, hydrogels with 10% and 13% starch concentrations demonstrated that the cross-linking structure phase in the CE isolation method forms hydrogels with a firm structure (Figure 5c).

The formation of the hydrogel structure is influenced by amylose as a linear chain and amylopectin as a branched chain. During gelatinization, amylopectin expands into a large gel-like structure, often referred to as a "gel-ball" or "super-globe," while amylose diffuses out of the granule. During the freeze-thaw process, the amylose chains then cross-link through interactions between hydroxyl (O-H) groups, enhancing the gel network structure [39, 57, 58]. Cross-linking between the O-H groups of amylose in the freeze-thaw process occurs with the help of ice crystals that push the polymer chains to bond and reorganize during thawing [53]. Typically, the freeze-thaw method is used for OH-rich polymers such as polyvinyl alcohol [10–12], [59–61]. However, by tuning the process parameters, freeze-thaw can be used to synthesize OH-rich natural polymers such as starch. Several previous studies have developed freeze-thawed starch hydrogels by adding synthetic polymers or cross-linkers as reinforcement [39, 62, 63]. These taro starch hydrogels, with entirely natural polymers without synthetic polymer reinforcement, and non-toxic solvents and processes, successfully formed cross-linked hydrogels and porous hydrogel structures. Prior research has indicated that hydrogels with cross-linked and porous structures have the potential to be a delivery platform for nutraceuticals. Porosity determines the structural design of hydrogels, controlling nutraceuticals loading, diffusion pathways, and swelling kinetics. However, high porosity increases loading and accelerates release, compromising mechanical stability. Therefore, a balance between permeability and structural integrity is essential for reliable delivery performance [64].

Figure 6 shows the swelling degree analysis to confirm the quantitative results under the morphological analysis. The swelling degree is a critical characteristic for practical applications as a potential delivery matrix. The three phases of hydrogel formation are indicated by a blue background for the granular swelling phase, a green background for the potential cross-linked phase, and an orange background for the completely cross-linked phase. The granular swelling phases are shown by samples SM (7%, 10%) and AQ (7%, 10%), which can swell in less than 3 hours. The potential cross-linking phases are shown by AQ (13%), SM (13%), and CE (7%), which can swell up to 12 hours, while the cross-linking phases are shown by samples CE (10%, 13%), which can swell up to 24 hours.

Overall, cross-linking formation of hydrogel is influenced by: (1) starch content, especially amylose which is the main cross-linking factor of hydrogel structure, (2) impurities/ash content, which makes it more difficult for OH to bond, (3) protein, which can help cross-linking through electrostatic interaction, hydrogen bonding, and Van der Waals interaction [65, 66]. Samples prepared with the CE method showed the highest amylose content, allowing potential cross-linking to form at a concentration of 7%. Meanwhile, in samples with AQ and SM methods that show lower amylose levels than CE, potential cross-linking is formed at a starch concentration of 13%. Furthermore, the high protein levels and low ash content affect the process of hydrogel cross-linking in CE samples.

The whiteness of taro starch hydrogels serves as an indicator of the purity of starch. It can validate the test results on the ability of hydrogel formation. Color analysis is crucial in the food industry as it helps determine the freshness, ripeness, diversity, and appeal of food products, ultimately leading to higher consumer acceptability [67, 68]. Starch whiteness corresponds to amylose content [39] and is a sensory color characteristic that the industry desires [69]. Figure 7 shows the highest whiteness level in the CE sample at 163.34, followed by AQ and SM at 143.45 and 132.24, respectively. This is directly proportional to the amylose content shown in Table 1. The amylose chain is a linear structure that prevents the formation of colors or other substances that cause a decrease in whiteness [69].

3.3 Texture Properties of Taro Starch Hydrogel

The textural properties of taro starch hydrogels were characterized using dried hydrogels (Table 5). Hardness is the mechanical resistance of a material, while fracturability is the ability of a material to crack or crumble. Both parameters increased in hydrogels with concentrations of 7% and 10% while decreasing at 13%. The decrease in hardness and

Table 5. Texture properties of hydrogel with variation concentration of taro starch.

Parameter	CE–7%	CE–10%	CE–13%
Hardness (gForce)	1559.25 ± 157.56^{ab}	1752.13 ± 255.86^{b}	855.70 ± 41.29^{a}
Fracturability (gForce)	885.24 ± 953.92^{a}	2244.02 ± 799.75^{a}	749.64 ± 222.91^{a}
Springiness (%)	0.07 ± 0.10^{a}	0.68 ± 0.58^{a}	0.41 ± 0.45^{a}
Cohesiveness (%)	0.31 ± 0.44^{a}	0.14 ± 0.01^{a}	0.11 ± 0.09^{a}
Gumminess (gForce)	445.56 ± 630.70^{a}	252.63 ± 51.79^{a}	98.26 ± 82.26^{a}
Chewiness (gForce)	60.39 ± 85.41^{a}	156.02 ± 110.95^{a}	58.65 ± 78.01^{a}
Resilience (%)	0.62 ± 0.88^{a}	0.17 ± 0.07^{a}	0.05 ± 0.03^{a}

fracturability was caused by excessive glucose unit length in taro starch amylose and inhibited the O-H cross-linking process [39]. The observation indicates that the weight loss was lower when the concentration of taro starch was 13% compared to 10% (Figure 4). The decrease in weight loss signifies a degradation of the hydrogel's ability to retain its form [9]. Likewise, chewiness and springiness, which are related to the elasticity of the hydrogel, decreased at 13% concentration. The decrease in these parameters was confirmed by the results of the swelling degree test in Figures 4a-b, which show an up-and-down graph (unstable) during the 24-hour test. The swelling degree is the ability of cross-links to stretch (elasticity) and is influenced by water trapped in the pores of the hydrogel structure [39, 70]. However, the cohesiveness, gumminess, and resilience reduced as the concentration of taro starch. The decrease in these parameters is attributed to the elevated concentration of taro starch, which inhibits granular swelling and consequently prevents cross-link formation in the hydrogel network structure. The gel network structure is weaker after the concentration is increased. The findings align with prior studies [26], indicating that elevating the corn starch concentration reduced cohesiveness, gumminess, and resilience.

The texture properties of the taro starch hydrogel obtained in this study showed distinctive characteristics compared to other natural and starch-based polymer hydrogels reported in several previous studies. Wu et al. (2017) reported that the hardness of quinoa and corn starch hydrogels was 201–900 g and around 721 g, respectively [71]. Additionally, the hardness of pea starch hydrogels with alcohol solvents is 928–1696 g [72]. The hardness of taro starch hydrogels reached 855–1752 g, indicating that hydrogels can achieve greater cross-linking stiffness. Regarding chewiness [15], corn starch hydrogels with xanthan gum or sodium alginate reported values between 30–164 g, while taro starch hydrogels were in the 58–156 g range. Taro starch hydrogels synthesized using the freeze-thaw method without adding other polymer reinforcements and toxic solvents showed comparable mastication resistance to composite hydrogels. Thus, taro starch has the potential as a single biopolymer for hydrogel formation, offering a simpler and more environmentally friendly alternative with competitive texture performance and good structural integrity.

4. CONCLUSION

This research analyzes taro starch using various isolation methods to determine its effect on hydrogel formation, starting from the phases of granule formation, potential cross-linking, and cross-linking, ultimately producing a firm hydrogel structure. Starch paste properties influence hydrogel formation, demonstrating a linear increase in PV, HV, FV, BV, and SV values as the starch content increases. The freeze-thaw parameters were optimized by freezing the sample for 17 hours at a temperature of -23°C and subsequently thawing it for 7 hours at a temperature of 4°C. We analyzed the effect of the taro starch isolation method and concentration on hydrogel formation using optical microscopy, SEM, swelling degree test, color analysis, and TPA test. The CE isolation method with the highest amylose content, the highest protein content, and the lowest impurities or ash content resulted in the firmest hydrogel structure. Meanwhile, the CE starch concentration of 10% produced the highest swelling degree and the lowest weight loss. The textural properties test at 10% CE starch concentration confirmed the firm structure of taro starch hydrogel. Physical properties demonstrated the cross-linking structure and dense, porous surface of the taro starch hydrogels. Thus, the formation process of taro starch hydrogels in this study has the potential for synthesizing environmentally friendly, freeze-thaw hydrogels. These hydrogels are beneficial as a delivery platform of nutraceuticals for edible matrices in future applications.

DATA AVAILABILITY STATEMENT

The datasets generated during and/or analyzed during the current study are available from the corresponding author on reasonable request.

CONFLICT OF INTEREST

The authors declare that there are no conflicts of interest associated with this publication, and there has been no significant financial support for this work that could have influenced its outcome.

ACKNOWLEDGMENTS

This research was financially supported by the Directorate of Research and Community Engagement, Institut Teknologi Bandung, under the "ITB Research Program" (Program Riset ITB) Grant in the fiscal years 2024-2025.

REFERENCES

[1] P. J. Matthews, M. E. Ghanem, Perception gaps that may explain the status of taro (colocasia esculenta) as an 'orphan crop', Plants, People, Planet 3 (2) (2021) 99–112. https://doi.org/10.1002/ppp3.10155.

[2] T. Mabhaudhi, et al., Prospects of orphan crops in climate change, Planta 250 (2019) 695–708. https://doi.org/10.1007/s00425-019-03129-y.

[3] R. Singh, S. Choudhary, A. K. Verma, Y. R., Taro (colocasia esculenta (l.) schoff.) for nutritional security and health benefits, in: Horticulture for Nutrition and Income Security, NIPA (New India Publisher Agency), New Delhi, India, 2023.

[4] X. Li, R. Yadav, K. H. M. Siddique, Neglected and underutilized crop species: the key to improving dietary diversity and fighting hunger and malnutrition in asia and the pacific, Frontiers in Nutrition 7 (2020) 593711. https://doi.org/10.3389/fnut.2020.593711.

[5] Aditikia, B. Kapoor, S. Singh, P. Kumar, Others, Taro (colocasia esculenta): Zero wastage orphan food crop for food and nutritional security, South African Journal of Botany 145 (2022) 157–169. https://doi.org/10.1016/j.sajb.2021.08.014.

[6] K. H. M. Siddique, X. Li, K. Gruber, Rediscovering asia's forgotten crops to fight chronic and hidden hunger, Nature Plants 7 (2) (2021) 116–122. https://doi.org/10.1038/s41477-021-00850-z.

[7] Grand View Research, Functional foods market size, share & trends analysis report by ingredient (carotenoids, prebiotics & probiotics, fatty acids, dietary fibers), by product, by application, by region, and segment forecasts, 2022–2030, https://www.grandviewresearch.com/industry-analysis/functional-food-market, market Analysis Report (2022).

[8] M. N. Saqib, B. M. Khaled, F. Liu, F. Zhong, Hydrogel beads for designing future foods: Structures, mechanisms, applications, and challenges, Food Hydrocolloids for Health 2 (2022) 100073. https://doi.org/10.1016/j.fhfh.2022.100073.

[9] H. R. Luthfianti, et al., Physicochemical characteristics and antibacterial activities of freeze-thawed polyvinyl alcohol/andrographolide hydrogels, ACS Omega 8 (3) (2023) 2915–2930. https://doi.org/10.1021/acsomega.2c05110.

[10] W. X. Waresindo, H. R. Luthfianti, D. Edikresnha, T. Suciati, F. A. Noor, K. Khairurrijal, A freeze–thaw pva hydrogel loaded with guava leaf extract: physical and antibacterial properties, RSC Advances 11 (48) (2021) 30156–30171. https://doi.org/10.1039/D1RA04092H.

[11] D. Edikresnha, T. Suciati, Suprijadi, K. Khairurrijal, Freeze-thawed hydrogel loaded by *Piper crocatum* extract with in-vitro antibacterial and release tests, Journal of Materials Research and Technology 15 (2021) 17–36. https://doi.org/10.1016/j.jmrt.2021.07.151.

[12] K. Kusjuriansah, et al., Composite hydrogel of poly (vinyl alcohol) loaded by *Citrus hystrix* leaf extract, chitosan, and sodium alginate with in vitro antibacterial and release test, ACS Omega 9 (11) (2024) 13306–13322. https://doi.org/10.1021/acsomega.3c10143.

[13] N. Asy-Syifa, Kusjuriansah, W. X. Waresindo, D. Edikresnha, T. Suciati, K. Khairurrijal, The study of the swelling degree of the pva hydrogel with varying concentrations of pva, in: Journal of Physics: Conference Series, Vol. 2243, 2022, p. 012053. https://doi.org/10.1088/1742-6596/2243/1/012053.

[14] H. Zhang, F. Zhang, J. Wu, Physically crosslinked hydrogels from polysaccharides prepared by freeze–thaw technique, Reactive and Functional Polymers 73 (7) (2013) 923–928. https://doi.org/10.1016/j.reactfunctpolym.2012.12.014.

[15] C. Cui, et al., Recent advances in the preparation, characterization, and food application of starch-based hydrogels, Carbohydrate Polymers 291 (2022) 119624. https://doi.org/10.1016/j.carbpol.2022.119624.

[16] P. Vithu, S. K. Dash, K. Rayaguru, M. K. Panda, M. Neduchezhiyan, Optimization of starch isolation process for sweet potato and characterization of the prepared starch, Journal of Food Measurement and Characterization 14 (3) (2020) 1520–1532. https://doi.org/10.1007/s11694-020-00401-8.

[17] T. Balcha, N. M. Josepha, A. Beletea, Isolation and physicochemical characterization of starch from taro boloso-i tubers, Indian Drugs 55 (7) (2018).

[18] F. Saputra, A. Hartiati, B. Admadi, Karakteristik mutu pati ubi talas (*Colocasia esculenta*) pada perbandingan air dengan hancuran ubi talas dan konsentrasi natrium metabisulfit, Jurnal Rekayasa dan Manajemen Agroindustri 4 (1) (2016) 62–71.

[19] S. Sonia, E. Julianti, R. Ridwansyah, The characteristic of taro flour based pasta with addition of modified starch and hydrocolloids, Indonesian Food and Nutrition Progress 16 (1) (2019) 27–35. https://doi.org/10.22146/ifnp.45681.

[20] C. K. Nagar, S. K. Dash, K. Rayaguru, U. S. Pal, M. Neduchezhiyan, Isolation, characterization, modification and uses of taro starch: A review, International Journal of Biological Macromolecules 192 (2021) 574–589. https://doi.org/10.1016/j.ijbiomac.2021.10.041.

[21] P. R. More, M. I. Talib, V. R. Parate, Development of modified instant starch from taro (*Colocasia esculenta*) by gelatinization, IOSR Journal of Environmental Science, Toxicology and Food Technology 11 (2017) 52–59. https://doi.org/10.9790/2402-1101025259.

[22] S. Simsek, S. N. El, Production of resistant starch from taro (*Colocasia esculenta* l. schott) corm and determination of its effects on health by in vitro methods, Carbohydrate Polymers 90 (3) (2012) 1204–1209. https://doi.org/10.1016/j.carbpol.2012.06.039.

[23] S. Sukhija, S. Singh, C. S. Riar, Isolation of starches from different tubers and study of their physicochemical, thermal, rheological and morphological characteristics, Starch–Stärke 68 (1–2) (2016) 160–168. https://doi.org/10.1002/star.201500186.

[24] E. Pérez, F. S. Schultz, E. P. de Delahaye, Characterization of some properties of starches isolated from *Xanthosoma sagittifolium* (tannia) and *Colocasia esculenta* (taro), Carbohydrate Polymers 60 (2) (2005) 139–145. https://doi.org/10.1016/j.carbpol.2004.11.033.

[25] N. Singh, J. Singh, L. Kaur, N. S. Sodhi, B. S. Gill, Morphological, thermal and rheological properties of starches from different botanical sources, Food Chemistry 81 (2) (2003) 219–231. https://doi.org/10.1016/S0308-8146(02)00416-8.

[26] W. Xiao, et al., Controlling the pasting, rheological, gel, and structural properties of corn starch by incorporation of debranched waxy corn starch, Food Hydrocolloids 123 (2022) 107136. https://doi.org/10.1016/j.foodhyd.2021.107136.

[27] R. N. Tharanathan, Biodegradable films and composite coatings: past, present and future, Trends in Food Science & Technology 14 (3) (2003) 71–78. https://doi.org/10.1016/S0924-2244(02)00280-7.

[28] R. K. Gupta, P. Guha, P. P. Srivastav, Exploring the potential of taro (colocasia esculenta) starch: Recent developments in modification, health benefits, and food industry applications, Food Bioengineering 3 (3) (2024) 365–379. https://doi.org/10.1002/fbe2.12103.

[29] J. B. Zhang, et al., Risk analysis of sulfites used as food additives in china, Biomedical and Environmental Sciences 27 (2) (2014) 147–154. https://doi.org/10.3967/bes2014.032.

[30] A. Sawitri, et al., Synthesis and characterization of novel electrospun nanofibers based on taro starch: influence of solvent and isolation agent on morphology and diameter, Polymer International (2024). https://doi.org/10.1002/pi.6709.

[31] S. S. Behera, R. C. Ray, Nutritional and potential health benefits of konjac glucomannan, a promising polysaccharide of elephant foot yam, *Amorphophallus konjac* k. koch: A review, Food Reviews International 33 (1) (2017) 22–43. https://doi.org/10.1080/87559129.2015.1137310.

[32] A. Ahmed, F. Khan, Extraction of starch from taro (*Colocasia esculenta*) and evaluating it and further using taro starch as disintegrating agent in tablet formulation with over all evaluation, inven. Rapid Nov. Excipients, 2013, 2:1–5 (2013).

[33] W. X. Waresindo, H. Rahmi, A. Priyanto, Freeze–thaw hydrogel fabrication method: basic principles, synthesis parameters, properties, and biomedical applications, Materials Research Express 10 (024003) (2023). https://doi.org/10.1088/2053-1591/acb98e.

[34] I. Palabiyik, O. S. Toker, S. Karaman, Ö. Yildiz, A modeling approach in the interpretation of starch pasting properties, Journal of Cereal Science 74 (2017) 272–278. https://doi.org/10.1016/j.jcs.2017.02.008.

[35] Z. Chen, et al., Skewed distribution of leaf color rgb model and application of skewed parameters in leaf color description

model, Plant Methods 16 (2020) 1–8. https://doi.org/10.1186/s13007-020-0561-2.

[36] X. Zhu, W. Cui, E. Zhang, J. Sheng, X. Yu, F. Xiong, Morphological and physicochemical properties of starches isolated from three taro bulbs, Starch–Stärke 70 (1–2) (2018) 1700168. https://doi.org/10.1002/star.201700168.

[37] M.-G. Dorantes-Fuertes, M. C. López-Méndez, G. Martínez-Castellanos, R. Á. Meléndez-Armenta, H.-E. Jiménez-Martínez, Starch extraction methods in tubers and roots: a systematic review, Agronomy 14 (4) (2024) 865. https://doi.org/10.3390/agronomy14040865.

[38] O. Paramita, S. Fathonah, Rosidah, T. Agustina, M. Larasati, The effect of different processes of flour making on the proximate composition of taro (colocasia esculenta l.) flour and taro flour cookies, IOP Conference Series: Earth and Environmental Science 700 (1) (2021) 012065. https://doi.org/10.1088/1755-1315/700/1/012065.

[39] B. Biduski, et al., Starch hydrogels: The influence of the amylose content and gelatinization method, International Journal of Biological Macromolecules 113 (2018) 443–449. https://doi.org/10.1016/j.ijbiomac.2018.02.144.

[40] C. D. Bet, C. S. de Oliveira, C. Beninca, T. A. D. Colman, L. G. Lacerda, E. Schnitzler, Influence of the addition of hydrocolloids on the thermal, pasting and structural properties of starch from common vetch seeds (*Vicia sativa* sp), Journal of Thermal Analysis and Calorimetry 133 (1) (2018) 549–557. https://doi.org/10.1007/s10973-018-7094-1.

[41] X. Yu, Y. Zhang, L. Ran, W. Lu, E. Zhang, F. Xiong, Accumulation and physicochemical properties of starch in relation to eating quality in different parts of taro (colocasia esculenta) corm, International Journal of Biological Macromolecules 194 (2022) 924–932. https://doi.org/10.1016/j.ijbiomac.2021.11.147.

[42] W. Liang, et al., Investigating the influence of $cacl_2$ induced surface gelatinization of red adzuki bean starch on its citric acid esterification modification: Structure–property related mechanism, Food Chemistry 436 (2024) 137724. https://doi.org/10.1016/j.foodchem.2023.137724.

[43] B. Karakelle, N. Kian-Pour, O. S. Toker, I. Palabiyik, Effect of process conditions and amylose/amylopectin ratio on the pasting behavior of maize starch: A modeling approach, Journal of Cereal Science 94 (2020) 102998. https://doi.org/10.1016/j.jcs.2020.102998.

[44] Y. Xiao, et al., Effect of different *Mesona chinensis* polysaccharides on pasting, gelation, structural properties and *in vitro* digestibility of tapioca starch–*Mesona chinensis* polysaccharides gels, Food Hydrocolloids 99 (2020) 105327. https://doi.org/10.1016/j.foodhyd.2019.105327.

[45] B. Shafie, S. C. Cheng, H. H. Lee, P. H. Yiu, Characterization and classification of whole-grain rice based on rapid visco analyzer (rva) pasting profile, International Food Research Journal 23 (5) (2016).

[46] A. Kaur, N. Singh, R. Ezekiel, H. S. Guraya, Physicochemical, thermal and pasting properties of starches separated from different potato cultivars grown at different locations, Food Chemistry 101 (2) (2007) 643–651. https://doi.org/10.1016/j.foodchem.2006.01.054.

[47] S. Varavinit, S. Shobsngob, W. Varanyanond, P. Chinachoti, O. Naivikul, Effect of amylose content on gelatinization, retrogradation and pasting properties of flours from different cultivars of thai rice, Starch–Stärke 55 (9) (2003) 410–415. https://doi.org/10.1002/star.200300185.

[48] B. Wang, et al., Structural changes in corn starch granules treated at different temperatures, Food Hydrocolloids 118 (2021) 106760. https://doi.org/10.1016/j.foodhyd.2021.106760.

[49] H. Dun, H. Liang, S. Li, B. Li, F. Geng, Influence of an o/w emulsion on the gelatinization, retrogradation and digestibility of rice starch with varying amylose contents, Food Hydrocolloids 113 (2021) 106547. https://doi.org/10.1016/j.foodhyd.2020.106547.

[50] A. A. Wani, P. Singh, M. A. Shah, U. Schweiggert-Weisz, K. Gul, I. A. Wani, Rice starch diversity: Effects on structural, morphological, thermal, and physicochemical properties—a review, Comprehensive Reviews in Food Science and Food Safety 11 (5) (2012) 417–436. https://doi.org/10.1111/j.1541-4337.2012.00193.x.

[51] R. Juhász, A. Salgó, Pasting behavior of amylose, amylopectin and their mixtures as determined by rva curves and first derivatives, Starch–Stärke 60 (2) (2008) 70–78. https://doi.org/10.1002/star.200700634.

[52] H. R. Luthfianti, et al., Bioactive compounds-loaded polyvinyl alcohol hydrogels: Advancements in smart delivery media for biomedical applications, Materials Research Express 11 (2024) 062002. https://doi.org/10.1088/2053-1591/ad4fdd.

[53] J. Tavakoli, J. Gascooke, N. Xie, B. Z. Tang, Y. Tang, Enlightening freeze–thaw process of physically cross-linked poly(vinyl alcohol) hydrogels by aggregation-induced emission fluorogens, ACS Applied Polymer Materials 1 (6) (2019) 1390–1398. https://doi.org/10.1021/acsapm.9b00173.

[54] M. Moghadam, M. S. S. Dorraji, F. Dodangeh, H. R. Ashjari, S. N. Mousavi, M. H. Rasoulifard, Design of a new light curable starch-based hydrogel drug delivery system to improve the release rate of quercetin as a poorly water-soluble drug, European Journal of Pharmaceutical Sciences 174 (2022) 106191. https://doi.org/10.1016/j.ejps.2022.106191.

[55] Y. Poyraz, N. Baltacı, G. Hassan, O. Alayoubi, B. Ö. Üysal, Ö. Pekcan, Composite hydrogel of polyacrylamide/starch/gelatin as a novel amoxicillin delivery system, Gels 10 (10) (2024) 625. https://doi.org/10.3390/gels10100625.

[56] W. Zhang, H. Chen, J. Wang, Y. Wang, L. Xing, H. Zhang, Physicochemical properties of three starches derived from potato, chestnut, and yam as affected by freeze–thaw treatment, Starch/Staerke 66 (3–4) (2014) 353–360. https://doi.org/10.1002/star.201200270.

[57] T. Jiang, Q. Duan, J. Zhu, H. Liu, L. Yu, Starch-based biodegradable materials: Challenges and opportunities, Advanced Industrial and Engineering Polymer Research 3 (1) (2020) 8–18. https://doi.org/10.1016/j.aiepr.2019.11.003.

[58] M. Sunyoto, M. Djali, A. F. Rizky, Study on the physical characteristics of macaroni made of cassava waste and corn flour by applying different sizes of die extruder and frequency of moulding, in: KnE Life Sciences, Vol. 2, 2017, p. 542. https://doi.org/10.18502/kls.v2i6.1074.

[59] M. Rodhiyah, et al., Exploring freeze-thawed cellulose-based hydrogel from corn cob: Physicochemical properties, antibacterial activity, and cytotoxicity assay, Biocatalysis and Agricultural Biotechnology 67 (2025) 103629. https://doi.org/10.1016/j.bcab.2025.103629.

[60] N. Nafisah, et al., Enhanced superabsorbency of cellulose-based hydrogels in naoh solution: Synthesis, characterization, and performance evaluation, in: Journal of Physics: Conference Series, Vol. 2734, 2024, p. 012036. https://doi.org/10.1088/1742-6596/2734/1/012036.

[61] W. X. Waresindo, H. Rahmi, A. Priyanto, et al., Extraction and characterization of glucomannan from young porang tubers (*Amorphophallus muelleri* blume) and its hydrogel formation for potential application in functional foods, Journal of Food Science and Technology (2025) 1–12https://doi.org/10.1007/s13197-025-06312-0.

[62] A. Hassan, M. B. K. Niazi, A. Hussain, S. Farrukh, T. Ahmad, Development of anti-bacterial pva/starch based hydrogel membrane for wound dressing, Journal of Polymers and the Environment 26 (1) (2018) 235–243. https://doi.org/10.1007/s10924-017-0944-2.

[63] C. Yu, X. Tang, S. Liu, Y. Yang, X. Shen, C. Gao, Laponite crosslinked starch/polyvinyl alcohol hydrogels by freezing/thawing process and studying their cadmium ion absorption, International Journal of Biological Macromolecules 117 (2018) 1–6. https://doi.org/10.1016/j.ijbiomac.2018.05.159.

[64] A. Dafe, H. Etemadi, A. Dilmaghani, G. R. Mahdavinia, Investi-

gation of pectin/starch hydrogel as a carrier for oral delivery of probiotic bacteria, International Journal of Biological Macromolecules 97 (2017) 536–543. https://doi.org/10.1016/j.ijbiomac.2017.01.060.

[65] Q. Zhang, Y. Liu, G. Yang, H. Kong, L. Guo, G. Wei, Recent advances in protein hydrogels: From design, structural and functional regulations to healthcare applications, Chemical Engineering Journal 451 (2023) 138494. https://doi.org/10.1016/j.cej.2022.138494.

[66] H. Li, N. Kong, B. Laver, J. Liu, Hydrogels constructed from engineered proteins, Small 12 (8) (2016) 973–987. https://doi.org/10.1002/smll.201502429.

[67] D. Wu, D.-W. Sun, Colour measurements by computer vision for food quality control—a review, Trends in Food Science & Technology 29 (1) (2013) 5–20. https://doi.org/10.1016/j.tifs.2012.08.004.

[68] P. S. Hornung, et al., Enhancement of the functional properties of dioscoreaceas native starches: Mixture as a green modification process, Thermochimica Acta 649 (2017) 31–40. https://doi.org/10.1016/j.tca.2017.01.006.

[69] J. Roźnowski, L. Juszczak, B. Szwaja, I. Przetaczek-Roźnowska, Effect of esterification conditions on the physicochemical properties of phosphorylated potato starch, Polymers (Basel) 13 (15) (2021) 2548. https://doi.org/10.3390/polym13152548.

[70] J. F. Douglas, F. Horkay, Influence of swelling on the elasticity of polymer networks cross-linked in the melt state: Test of the localization model of rubber elasticity, The Journal of Chemical Physics 160 (22) (2024). https://doi.org/10.1063/5.0212901.

[71] G. Wu, C. F. Morris, K. M. Murphy, Quinoa starch characteristics and their correlations with the texture profile analysis (tpa) of cooked quinoa, Journal of Food Science 82 (10) (2017) 2387–2395. https://doi.org/10.1111/1750-3841.13848.

[72] Y. Sun, et al., Gelatinization, pasting, and rheological properties of pea starch in alcohol solution, Food Hydrocolloids 112 (2021) 106331. https://doi.org/10.1016/j.foodhyd.2020.106331.

